High refractive index properties of oxyfluorosilicate glasses and a unified dielectric model of silicate oxide glasses in the sub-terahertz frequency region

Wada, Osamu
Ramachari, Doddoji
Yang, Chan-Shan
Uchino, Takashi
Pan, Ci-Ling

(Citation)
Optical Materials Express,10(2):607-621

(Issue Date)
2020-01-28

(Resource Type)
journal article

(Version)
Version of Record

(URL)
https://hdl.handle.net/20.500.14094/90008125

Research Article | Vol. 10, No. 2 / 1 February 2020 / Optical Materials Express 607
Optical Materials EXPRESS

High refractive index properties of oxyfluorosilicate glasses and a unified dielectric model of silicate oxide glasses in the sub-terahertz frequency region

Osamu Wada,[1,2,7] Doddoji Ramachari,[1,6] Chan-Shan Yang,[3,4] Takashi Uchino,[5] and Ci-Ling Pan[1,8]

[1]*Department of Physics, National Tsing Hua University, Hsinchu 30013, Taiwan*
[2]*Office for Academic and Industrial Innovation (Oacis), Kobe University, Kobe 657-8501, Japan*
[3]*Institute of Electro-Optical Engineering, National Taiwan Normal University, Taipei 11677, Taiwan*
[4]*Undergraduate Program of Electro-Optical Engineering, National Taiwan Normal University, Taipei 11677, Taiwan*
[5]*Graduate School of Science, Kobe University, Kobe 657-8501, Japan*
[6]*Institute of Research and Development, Duy Tan University, Da Nang 550000, Vietnam*
[7]*fwga3962@nifty.com*
[8]*clpan@phys.nthu.edu.tw*

Abstract: Dielectric properties of oxyfluorosilicate (OFS) glasses have been characterized using Terahertz (THz)-time domain spectroscopy in the sub-THz region as well as optical reflection measurement. OFS glass containing 20 mol% of Nb_2O_5, which is termed ZNbKLSNd glass, has the highest refractive index of 3.70 in the sub-THz region. The THz and optical refractive indices of various silicate oxide glasses, including OFS glasses, have been confirmed to be correlated by a unified relationship utilizing a parameter defined by the ratio of ionic to electronic polarizability. Additionally, the frequency dependence of the THz dielectric constant has been interpreted by a single oscillator model for all silicate oxide glasses including OFS glasses. On the basis of the present unified dielectric model, the very high refractive index of ZNbKLSNd glass has been attributed to the lowering of oscillator resonance wavelength originated from the incorporation of Nb_2O_5 intermediate network former.

1. Introduction

Terahertz (THz) wave technology, which typically covers a frequency range of sub-THz to tens-THz, is demanded for the applications to a variety of systems including spectroscopy, communications, sensing and imaging due to the characteristic transmission and propagation properties of THz waves in various media [1–3]. Recent developments are widening the application field to cover materials, telecommunications, and variety of equipments in production, bio-medicine, environment, security, etc. [4–6]. In constructing practical THz and sub-THz components and systems, glasses are indispensable materials. Particularly, glasses having high-refractive index and low-loss properties are prerequisite for forming basic passive components such as lenses and waveguides as well as active components based on high nonlinearity of glasses in the THz and sub-THz regions [7,8]. If empirical Miller's rule [9,10] can be applied in the THz range, high refractive index glasses are also expected to exhibit a high nonlinearity, which merits their application to THz nonlinear functions including modulation, switching and wavelength conversion [11–13].

So far, a variety of silicate oxide glasses with metal oxide modifiers and chalcogenide glasses which have high chemical/mechanical stability and desirable dielectric properties, e.g., high refractive index, high transparency and high optical nonlinearity, have been developed for the

#382686 https://doi.org/10.1364/OME.382686
Journal © 2020 Received 8 Nov 2019; revised 8 Jan 2020; accepted 15 Jan 2020; published 28 Jan 2020

Optical Materials EXPRESS

application in visible and mid-infrared wavelength regions [14,15]. Investigation on dielectric properties of glass materials in the THz frequency range has first been carried out by means of far-infrared absorption measurements, and fairly limited kinds of glasses such as fused silica, soda-lime glass and As-S/Se glasses have been studied [16–20]. Detailed studies on THz dielectric properties have been started fairly recently by using THz-time domain spectroscopy (THz-TDS) technique on various materials [21–24]. The use of THz-TDS technique has been extended to detailed characterization of a variety of glass materials such as silicate oxides [25–28] and chalcogenides [29–31]. Naftaly has reported a study of THz refractive index and absorption properties of a series of commercial silicate oxide glasses and found their relationships with the optical refractive index and other various material properties including the density and thermal expansion coefficient [27]. Ravagli has carried out a study on sub-THz refractive index and absorption coefficient in a selection of chalcogenide and La:chalcogenide glasses with varied compositions, and discussed the absorption mechanism [29]. We have recently conducted sub-THz characterization of oxyfluorosilicate (OFS) glasses as a new group of silicate oxide glasses [32], in which fluorides (ZnF_2, PbF_2 and LiF) and rare-earth ions (Nd^{3+}) are introduced in the silicate glass host, along with the incorporation of alkali ions (K^+ and Na^+) and/or metal oxide based intermediate network former (Nb_2O_5) on the basis of our previous studies on various OFS glasses [33,34]. An OFS glass containing 20 mol % of Nb_2O_5, which is termed ZNbKLSNd glass, has achieved the simultaneous realization of the highest refractive index and lowest absorption loss among silicate oxide glass family in sub-THz frequency region [32]. Comparative analysis of THz properties has indicated that the very low absorption loss achieved in OFS glass is attributed to the effect of fluorine to relax structural disordering, which reduces charge fluctuation and eventually minimizes the absorption loss in the glass.

In view of either applying existing glasses in practice or developing new glasses for advanced systems, it is essential to understand the mechanism of how the THz dielectric properties of those glasses are determined. However, there has been no fully comprehensive description of THz dielectric property even within the silicate oxide glass family.

In this study, we carry out detailed characterization of dielectric property of OFS glasses using the same glasses as used in our recent work [32]. THz dielectric properties of these glasses are analyzed by using THz-TDS data [32], and optical reflectivity measurement is performed for optical refractive index determination. We compare THz properties of these series of OFS glasses with those of different multicomponent silicate oxide glasses [27] and chalcogenide glasses, particularly La^{3+}:chalcogenides [29], for which detailed THz dielectric property data are available. For a comparative study, we first focus on the difference between the optical and THz refractive indices, from which the electronic and ionic polarizabilities are determined. This analysis gives a unified relationship between the optical and THz refractive indices for all the silicate oxide glasses examined. Next, we analyze the THz frequency dependence of refractive index using a single oscillator model, so that the characteristic oscillator parameters are determined for different glasses. While all those data confirm the validity of the single oscillator model, they also indicate the difference in characteristic parameters for different glass groups. We discuss possible mechanism behind the high THz refractive index properties of the present OFS glasses.

2. Experimental methods

2.1. Glass preparation

The OFS glass samples employed in our experiment involve two glass groups [32]; one is ZNbKLSNd: $(20\text{-}x)ZnF_2 + 20Nb_2O_5 + 20K_2CO_3 + 10LiF + 30SiO_2 + xNd_2O_3$, and the other is PbNKLSNd: $(20\text{-}x)PbF_2 + 5Na_2O + 20K_2CO_3 + 10LiF + 45SiO_2 + xNd_2O_3$, where $x = 1$, 5 and 10 mol%. Glasses were prepared by the melt-quenching technique [32]. A batch composition (weight: ~15 g) was thoroughly crushed in an agate mortar and the homogeneous mixture was

Optical Materials EXPRESS

taken into a platinum crucible and heated at 1250 °C for 3 hours in an ambient. The melt was then annealed at 400 °C for 10 hrs to remove thermal strains. After cooling down, glasses were polished and formed into disks with the thickness of ~ 1.6 mm for measurements.

2.2. Characterization and analyzing techniques

The THz optical constants of OFS glasses were determined by using a photoconductive-antenna-based transmission type THz-TDS system [3,24,32]. A Ti-sapphire laser (wavelength: 800 nm) with duration of 60 fs, average optical power of 380 mW was used for exciting GaAs photoconductive antennae for THz generation and detection in an ambient.

The THz electric fields were recorded in the time domain with ($E_{\mathrm{sam}}(t)$) and without ($E_{\mathrm{ref}}(t)$) the glass sample, which was placed in the collimated THz beam path of the THz-TDS system. By Fourier-transforming the measured time-domain electric field data, we then retrieved the complex amplitude and phase of the transmitted THz waves in the frequency domain. The THz refractive index $n(\nu)$ and extinction coefficient $\kappa(\nu)$ at the frequency ν are related to the electric field $E(\nu)$ and phase $\phi(\nu)$ measured after transmission through a reference (air in our case)(suffix: ref) and through the sample (suffix: sam) by the following equations [27];

$$n(\nu) = 1 + \frac{c}{2\pi\nu d}(\phi_{sam}(\nu) - \phi_{ref}(\nu)) \tag{1}$$

$$k(\nu) = \frac{\alpha(\nu)c}{4\pi\nu} = \frac{c}{2\pi\nu d}\ln\left(\left|\frac{E_{ref}(\nu)}{E_{sam}(\nu)}\right|\frac{[n(\nu)+1]^2}{4n(\nu)}\right), \tag{2}$$

where $\alpha(\nu)$ is the absorption coefficient at the frequency ν, c is the speed of light, and d is the glass thickness. The second term inside the natural logarithm of Eq. (2) is a Fresnel reflection correction factor, in which the extinction coefficient is ignored because of its negligible contribution in our glass samples. The effect of multiple reflections of THz wave within the sample is not included. Taking account of the THz refractive index of our samples greater than 2, the transit time of THz wave in our samples (d~1.6 mm) is greater than 11 ps, which is much longer than the THz pulse width (typically 2 ps) in the present THz-TDS system. Under this condition, the transmitted THz signal is not influenced severely by the multiple reflection effects, and equations shown above are relevantly used for characterization.

The optical transmission and reflectivity r were measured by using the conventional Fourier transform infrared (FTIR) spectroscopy system in the visible to near-infrared range. The optical refractive index n_{opt} was determined at the wavelength of 1.5 μm using the standard equation:

$$n_{opt} = \frac{1+\sqrt{r}}{1-\sqrt{r}}. \tag{3}$$

3. Results and discussions

3.1. THz refractive index and polarizability

Figure 1 shows the frequency dependence of the refractive index $n(\nu)$ and extinction coefficient $k(\nu)$ of OFS glasses determined in the frequency range from 0.2 to 0.8 THz by using the same original THz-TDS data as used in [32]. The extinction coefficient is found to be smaller by more than 40 times compared with the refractive index within the measured frequency range. General behavior of frequency dependence as observed here is consistent with those of previously reported oxide-based silicate and chalcogenide glasses in the sub-THz frequency band [27–30]. The refractive indices measured in the present glasses are comparatively high, and ZNbKLSNd glasses particularly exhibit refractive indices as high as 3.70, being the highest among silicate glasses reported to date and close to those of La^{3+}:chalcogenide glasses [32]. It should be reemphasized that the absorption coefficients ($\alpha(\nu)=4\pi\nu\kappa/c$) at 0.5 THz (5.6-8.7 cm^{-1} for ZNbKLSNd glasses

Optical Materials EXPRESS

and 7.6-8.9 cm^{-1} for PbNKLSNd glasses) are significantly low as compared with other high-refractive index glasses [32]. This is interpreted to be caused primarily due to the structural relaxation effect of fluorine in OFS glasses as discussed in our previous work [32]. Figure 2 shows the wavenumber/wavelength dependence of the optical reflection measured in the infrared region and the optical refractive index calculated by using Eq. (3) for both of OFS glasses. It is observed that the reflection and refractive index are nearly constant at the wavenumber greater than 4000 cm^{-1} (wavelength < 2.5 μm) in both OFS glasses, and we use the refractive index values at the wavelength of 1.5 μm as the optical refractive indices for later discussion. Table 1 summarizes the THz and optical refractive index data for the present OFS glasses as well as selected silicate oxide and chalcogenide glasses taken from Refs. [27,29]. The compositions of the glasses selected in Table 1 are listed together with respective Refs. [35–38], in Table 2.

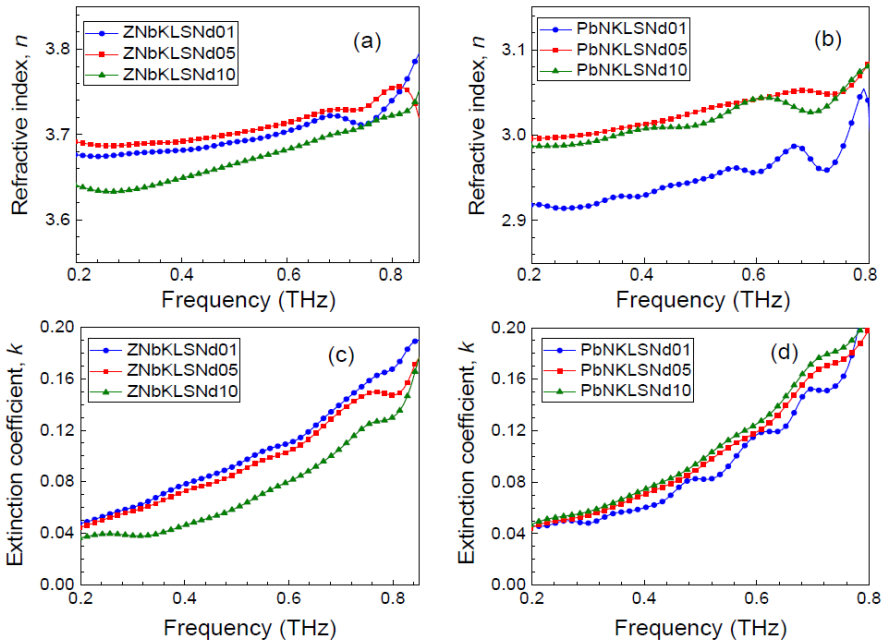

Fig. 1. Refractive index and extinction coefficient for (a),(c)ZNbKLSNd glasses and (b),(d) PbNKLSNd glasses determined by THz-TDS measurements.

In order to compare dielectric properties of the present OFS glasses with other silicate oxide and chalcogenide glasses, we analyze the data by using the Clausius-Mossotti equation (Lorentz-Lorentz equation) [27,32,39,40]. The dielectric constant ε_{opt} in the optical frequency range is determined by the polarizability of electrons associated with constituent molecules in the glass. On the other hand, the dielectric constant ε_{THz} in the sub-THz frequency range is determined by the total polarizability including contributions not only of fast response electrons (P_e) but also of slow response ions (P_i) in the glass. Thus the dielectric constants, ε_{opt} and ε_{THz}, are related to the molar electronic polarizability, P_e, molar ionic polarizability, P_i, and molar total polarizability, $P_{tot} = P_e + P_i$, as shown in the following relations:

$$\frac{\varepsilon_{opt} - 1}{\varepsilon_{opt} + 2} V_m = \frac{4\pi}{3} N_A P_e = R_m^e, \tag{4}$$

Optical Materials EXPRESS

Table 1. Material, THz, and optical parameters determined for a variety of glasses selected in the present analysis.

Glass	M (g/mol)	ρ (g/cm^3)	V_m (cm^3/mol)	n_{THz}	n_{opt}	P_{tot} (Å^3)	P_e (Å^3)	P_i (Å^3)	$a=P_i/P_e$	ε_{THz}-ε_{opt}	λ_0 (μm)	G (10^{10} cm/mol)	Ref.
ZNbKLSNd01	124	3.65	34.0	3.68	1.81	10.9	5.82	5.05	0.868	10.27	74.57	6.247	
ZNbKLSNd05	133	3.66	36.3	3.70	1.79	11.7	5.99	5.67	0.947	10.49	78.89	6.066	
ZNbKLSNd10	145	3.54	41.0	3.65	1.80	12.6	6.83	5.80	0.850	10.08	98.72	4.186	
PbNKLSNd01	110	3.72	29.7	2.95	1.57	8.47	3.79	4.68	1.24	6.24	126.5	1.279	
PbNKLSNd05	114	3.78	30.2	3.04	1.63	8.77	4.19	4.58	1.10	6.58	112.6	1.510	
PbNKLSNd10	119	3.62	32.8	2.96	1.53	9.38	3.94	5.44	1.38	6.42	115.5	1.617	
Silica	60	2.20	27.3	1.96	1.46	5.26	2.91	2.35	0.810	1.71			[27]
Pyrex	62	2.23	27.8	2.11	1.47	5.90	3.02	2.88	0.950	2.27			[27]
BK7	65	2.51	26	2.51	1.52	6.60	3.09	3.51	1.15	3.99	80.84	1.586	[27]
SK10	112	3.64	30.8	2.91	1.62	8.71	4.29	4.42	1.03	5.85	126.7	1.082	[27]
SF10	153	4.28	35.8	3.21	1.73	10.7	5.66	5.07	0.900	7.31	138.7	1.305	[27]
SF6	177	5.18	34.2	3.56	1.81	10.8	5.86	4.93	0.840	9.40	132.5	1.762	[27]
S1	61	4.27	14.3	3.89	2.37	4.60	3.38	1.22	0.361	9.52	108.8	1.110	[29]
S2	58	4.48	13.0	3.74	2.38	4.20	3.07	1.13	0.368	8.32	110.4	0.953	[29]
S3	56	4.11	13.6	3.60	2.37	4.30	3.22	1.08	0.335	7.34	95.68	1.064	[29]
S4	61	3.99	15.3	3.50	2.31	4.80	3.53	1.27	0.360	6.91	91.41	1.343	[29]
S5	65	4.21	15.4	3.65	2.37	4.90	3.65	1.25	0.343	7.71	93.09	1.343	[29]
S6	76	4.66	16.3	2.85	2.73	4.60	4.36	0.24	0.055	0.67	139.4	0.303	[29]
S7	82	4.41	18.6	3.19	2.60	5.60	4.79	0.81	0.169	3.42	139.7	0.052	[29]

Table 2. Compositions of a variety of glasses selected in the present analysis.

Glass	Composition	Ref.
ZNbKLSNdx	(20-x)ZnF_2+20Nb_2O_5+20K_2CO_3+10LiF + 30SiO_2 +$x$$Nd_2O_3$	
PbNKLSNdx	(20-x)PbF_2+5Na_2O + 20K_2CO_3+10LiF + 45SiO_2+ $x$$Nd_2O_3$	
Silica	SiO_2	[27]
Pyrex	80.6SiO_2+12.6B_2O_3+4.2Na_2O + 2.2Al_2O_3+0.04Fe_2O_3+0.1CaO + 0.05MgO + 0.1Cl	[35]
BK7	68.9SiO_2+10.1B_2O_3+8.8Na_2O + 8.4K_2O + 2.8BaO + 1.0As_2O_3	[36]
SK10	30.6SiO_2+11.7B_2O_3+5.0Al_2O_3+0.1Na_2O + 48.2BaO + 2.0ZnO + 0.7PbO + 0.8Sb_2O_3+0.9As_2O_3	[37]
SF10	35.3SiO_2+2.0Na_2O + 2.5K_2O + 55.7PbO + 4.0TiO_2+0.5As_2O_3	[37]
SF6	27.7SiO_2+0.5Na_2O + 1.0K_2O + 70.5PbO + 0.3As_2O_3	[38]
S1	$La_{20}Ga_{20}S_{60}$	[29]
S2	$La_{16}Ga_{24}S_{60}$	[29]
S3	$La_{12}Ga_{28}S_{60}$	[29]
S4	$La_{12}Ga_{28}S_{48}Se_{12}$	[29]
S5	$La_{12}Ga_{28}S_{39}Se_{21}$	[29]
S6	$Ge_{33}As_{12}Se_{55}$	[29]
S7	$Ge_{28}Sb_{12}Se_{60}$	[29]

Optical Materials EXPRESS

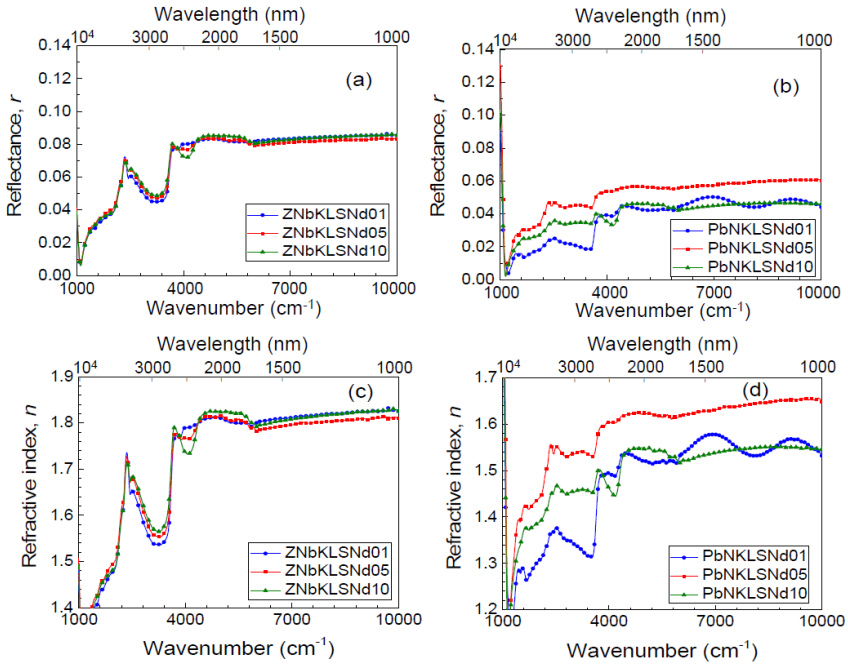

Fig. 2. Optical reflectance and refractive index spectra for (a),(c)ZNbKLSNd glasses and (b),(d) PbNKLSNd glasses.

$$\frac{\varepsilon_{THz}-1}{\varepsilon_{THz}+2}V_m = \frac{4\pi}{3}N_A(P_e+P_i) = R_m^{tot} = R_m^e(1+a), \tag{5}$$

where V_m is the molar volume defined by ρ/M using the density ρ and molecular weight M, N_A is the Avogadro number (6.023×10^{23} mol^{-1}), R_m^e is the molar electronic refraction, R_m^{tot} is the molar total refraction including both electronic and ionic contributions, and a is defined as a ratio P_i/P_e. Taking account of that the extinction coefficient ($k=\alpha c/(4\pi\nu)$) is negligibly small compared to the refractive index in the sub-THz region in those glasses, the dielectric constant ε_{THz} is obtained from $\varepsilon_{THz}=n_{THz}^2$. Similarly the optical dielectric constant ε_{opt} is obtained from $\varepsilon_{opt}=n_{opt}^2$. By using Eqs. (4) and (5), the polarizabilities can be determined from the measured refractive indices in each frequency range. The optical reflectivity spectra have been measured for OFS glasses as shown in Fig. 2(a) and (b), and then the refractive indices have been determined from them using Eq. (3), and the resultant spectra are shown in Fig. 2(c) and (d). The optical refractive indices determined at the wavelength of 1.5 μm are included in Table 1.

Figure 3 shows the total, electronic and ionic polarizabilities thus obtained as functions of the molar volume for the present OFS glasses, in which data for other silicate oxide and La:chalcogenide glasses (S1-S5 in Table 1 and 2) as well as other chalcogenide glasses (IG series) (S6, S7 in Tables 1 and 2) taken from the literature [27,29] are also plotted. The compositions of glasses used in Fig. 3 are listed in Table 2, and their physical and dielectric parameters are summarized in Table 1. The straight line in Fig. 3 shows a guide line corresponding to the THz refractive index of 3.7. THz plots of ZNbKLSNd glasses and La:chalcogenide glasses show a slope similar to this guide line being consistent with the THz refractive index very close to 3.7 as confirmed in Table 1.

In Fig. 3, it is found that the electronic and ionic contributions to the total polarizability are different for different glass groups; both contributions are comparable in silicate oxide glass

Optical Materials EXPRESS

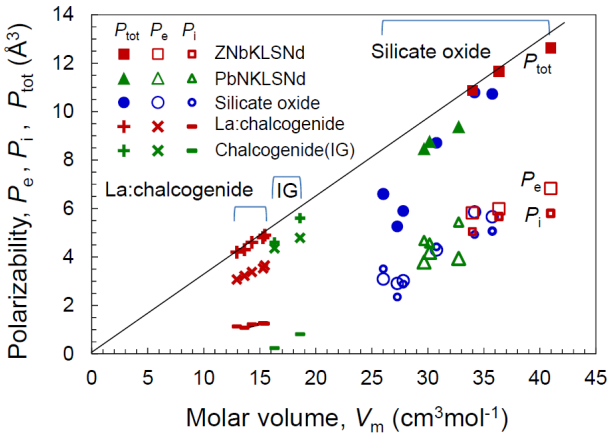

Fig. 3. Electronic, ionic and total molar polarizabilities versus molar volume for all glasses selected for the present comparison. A straight line indicates a slope corresponding to a refractive index of 3.70.

group, and electronic contribution is much larger than ionic contribution in chalcogenide glasses. This implies that the total polarizability of different glass systems is characterized in view of the ionic and electronic polarizability ratio which is defined by $a = P_i/P_e$. By using this ratio a, the electronic molar refraction R_m^e and the molar volume V_m, the optical refractive index (n_{opt}) and THz refractive index (n_{THz}) can be expressed by the following equations:

$$n_{opt} = \sqrt{\frac{1 + 2R_m^e/V_m}{1 - R_m^e/V_m}}, \tag{6}$$

$$n_{THz} = \sqrt{\frac{1 + 2R_m^e(1+a)/V_m}{1 - R_m^e(1+a)/V_m}}. \tag{7}$$

Figure 4 shows the relationships between the THz refractive index and optical refractive index for the silicate oxide glass group and La:chalcogenide glass group. Curves shown in the figure have been calculated from Eqs. (6) and (7) by using R_m^e/V_m as a parameter with assumptions of $a = 0.95$ for silicate oxide and $a = 0.35$ for La:chalcogenide glass groups, respectively. As seen in this result, different glass groups are classified by the polarizability ratio a. This classification applies to a variety of additives incorporated in the silicate oxide glasses. Slight deviation of the experimental data from the calculation is interpreted by considering an appropriate shift of a from 0.95, for example $a = 0.85$-0.95 for ZNbKLSNd glasses and $a = 1.10$-1.38 for PbNKLSNd glasses, as shown in Table 1. The same trend is observed for La:chalcogenide glass group. These results support the applicability of the polarizability ratio a in characterizing chemical composition/structure of the glass within the same glass family, e.g., silicate oxide glasses in which the oxygen ion O^{2-} governs the dielectric property. Naftaly et al. reported a linear relationship between the optical and THz refractive indices in high-refractive index silicate oxide glasses, but the linear relationship does not hold for low-refractive index glasses such as Pyrex and fused silica [27]. This allows us to confirm that the polarizability ratio a is useful to characterize dielectric properties of glasses with a wider range of compositions.

Optical Materials EXPRESS

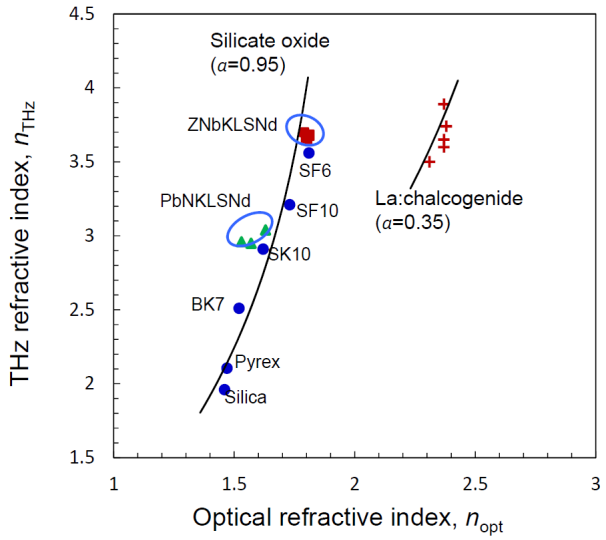

Fig. 4. Relationship of THz refractive index as functions of optical refractive index for various glasses. Curves shown have been calculated by using Eqs. (6) and (7) for fixed values of $a = P_i/P_e$.

3.2. *Ionic contribution to the dielectric characteristics of silicate oxide glasses*

In the previous section we have shown that the electronic and ionic contributions to the dielectric properties are correlated by a unified relationship for all silicate oxide glasses. In the following, we focus on the ionic contribution to the dielectric property and discuss its relation with physical properties of glasses. In the present analysis, we adopt a simplified model of dielectric material. The dielectric constant (ε) at a given frequency (ν) in the THz and far-infrared (FIR) region, ε_ν, is assumed to be expressed by the classical single oscillator model (Lorentz model) for displacement of a pair of anion and cation as shown by the following equation [40–42]:

$$\varepsilon_\nu = \varepsilon_\infty + \frac{4\pi N e^2}{\mu} \frac{f}{\nu_0^2 - \nu^2 - i\gamma\nu}, \tag{8}$$

where ε_∞ is the dielectric constant at the infinite frequency ($\nu = \infty$), e is the electronic charge, μ is the reduced mass of ions given by $1/\mu = 1/m_+ + 1/m_-$, where m_+ and m_- are the masses of anion and cation, N is the number of unit cells involving ion pairs per unit volume, ν_0 is the resonance frequency of the oscillator, f is the oscillator strength, and γ is the damping factor for displacement. We assume here single charge anion and cation for simplicity; that is, a single parameter ν_0 will represent the resonance frequency of the oscillator and will effectively determine dielectric characteristics in the THz to sub-THz frequency range. Since we are interested in dielectric property in the sub-THz range, which is much lower than the resonance frequency, the damping factor can be neglected in Eq. (8). For further analysis, we rewrite Eq. (8) to express the dielectric constant as a function of the wavelength λ, e(l), in the following form:

$$\frac{1}{\varepsilon(\lambda) - \varepsilon(0)} = \frac{\pi c^2 \mu V_m}{N_A e^2 f} \left(\frac{1}{\lambda_0^2} - \frac{1}{\lambda^2} \right), \tag{9}$$

Optical Materials EXPRESS

where $N = N_A/V_m$ and the oscillator resonance wavelength λ_0 have been used. When we define a material dependent amplitude factor g as:

$$g = \frac{N_A e^2 f}{\pi c^2 \mu}, \tag{10}$$

Equation (9) can be written as:

$$\frac{1}{\varepsilon(\lambda) - \varepsilon(0)} = \frac{V_m}{g}\left(\frac{1}{\lambda_0^2} - \frac{1}{\lambda^2}\right). \tag{11}$$

This indicates that a plot of $1/[\varepsilon(\lambda) - \varepsilon(0)]$ as a function of $1/\lambda^2$ gives a straight line, and its slope gives the value of g through $g = V_m/[\text{slope}]$. Considering the y-intercept $1/[\varepsilon(\lambda) - \varepsilon(0)]$ of this plot for $\lambda \rightarrow \infty$, Eq. (11) leads to the following relation:

$$\varepsilon(\infty) - \varepsilon(0) = \frac{g\lambda_0^2}{V_m}. \tag{12}$$

Therefore [slope]/[y-intercept] yields the value of ${\lambda_0}^2$ for each of the glass material.

In the present analysis, the values of $\varepsilon(0)$ have been determined from the refractive indices measured at the optical wavelength (λ=1.5 μm) by using the relation $\varepsilon(0) = \varepsilon_{opt} = n_{opt}^2$. For $\varepsilon(\infty)$, we have used the value of $\varepsilon(0.2\text{THz}) = \varepsilon_{THz} = n_{THz}^2$ since $\varepsilon(\lambda)$ virtually saturates at 0.2 THz (Fig. 1). Figure 5 shows $1/[\varepsilon(\lambda) - \varepsilon(0)]$ as functions of $1/\lambda^2$ for ZNbKLSNdx (x = 1, 5, 10) and PbNKLSNdx (x = 1, 5, 10) glass series, which show good linear dependences. The g factor and λ_0 are readily determined from these graphs, and the results are included in Table 1. The same analysis has been carried out for other silicate oxide glass groups by using the data reported in the literature [27]. Figure 6 shows plots of selected silicate oxide glasses. Some THz-TDS data show weak frequency dependences (e.g. silica and Pyrex) and those data have been excluded for accuracy in the present analysis. All data plotted in Fig. 6 show linear relationships and the values of g and λ_0 determined for all glasses (including La:chalcogenide glasses) are listed in Table 1.

Figures 5 and 6 show that THz dielectric properties of all glasses analyzed here can be interpreted by the single oscillator model. Equation (12) indicates that $\varepsilon(\infty) - \varepsilon(0)$, which corresponds to the ionic contribution to the dielectric constant, is governed by V_m, g and λ_0 all of which are characteristic to each glass material. To see the ionic contribution in different glass groups, we plot the dielectric constant difference $\varepsilon_{THz} - \varepsilon_{opt}$ .as a function of $g{\lambda_0}^2/V_m$ in Fig. 7. Here we use $\varepsilon(\nu = 0.2\text{ THz})$ for the ε_{THz} value for determining the dielectric constant difference, and all parameters are determined basically from the experimental data as described above. As is seen clearly in Fig. 7, a linear relationship has been obtained without regard to the difference of glass groups (including La:chalcogenide glasses: not shown). This confirms a wide applicability of the single oscillator model for characterizing THz dielectric properties of all glass materials examined.

Next question is what parameters are governing the overall dielectric property in each glass. In order to find out such dominant parameters, $\varepsilon_{THz} - \varepsilon_{opt}$ has been plotted as functions of each parameter: $1/V_m$, g and ${\lambda_0}^2$, as shown in Fig. 8. Here $1/V_m$ is regarded to be proportional to the number of ion pairs in a unit volume. Other parameters, g and ${\lambda_0}^2$, are used to characterize nature of the oscillator. As shown in Fig. 8(a), over a wide range of variation in the dielectric constant difference, $1/V_m$ does not show too much change. In contrast, Fig. 8(b) and (c) show that the dielectric constant difference increases in proportion to g as well as ${\lambda_0}^2$, which is consistent with the indication of Eq. (12). If we look into these g and ${\lambda_0}^2$ dependences more closely, they can be categorized into two classes: ZNbKLSNd glasses, and all other silicate oxide glasses.

Optical Materials EXPRESS

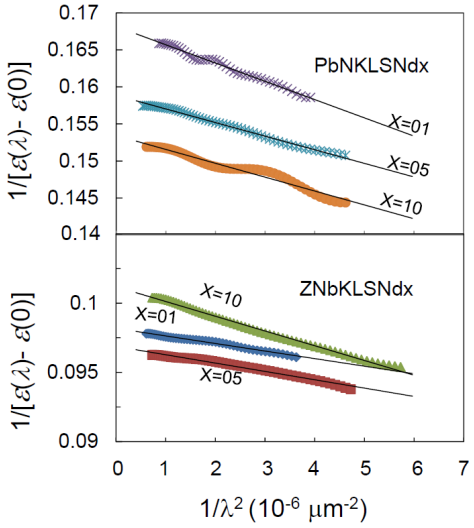

Fig. 5. $1/[\varepsilon(\lambda)- \varepsilon(0)]$ versus $1/\lambda^2$ plots for ZNbKLSNd and PbNKLSNd glasses with different compositions.

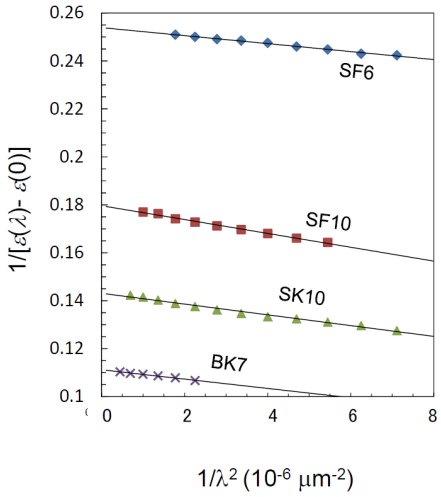

Fig. 6. $1/[\varepsilon(\lambda)- \varepsilon(0)]$ versus $1/\lambda^2$ plots for four silicate oxide glasses.

Optical Materials EXPRESS

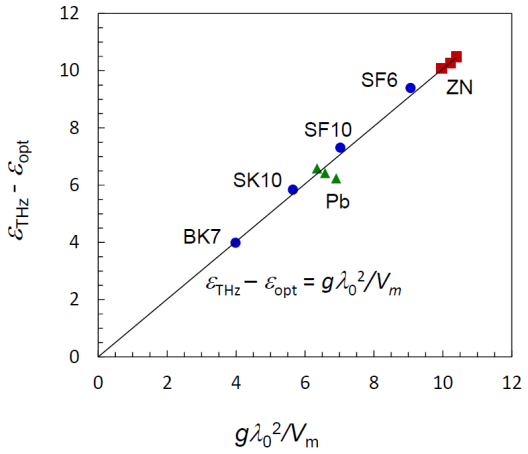

Fig. 7. Relationship between ε_{THz} - ε_{opt} versus $g\lambda_0^2/V_m$ for selected chalcogenide and silicate oxide glasses. Plots show experimental data determined from the single oscillator analysis and the straight line shows a slope of unity.

A distinct difference is observed between these classes. In ZNbKLSNd glasses, the very large dielectric constant difference (>10) is achieved by the large value of g (rather than by λ_0^2). By contrast, in other silicate oxide glasses including PbNKLSNd glasses, the increase of the dielectric constant difference is caused by the increase of λ_0^2 (rather than of g). Thus the present single oscillator model analysis has revealed that the different physical parameter is responsible for the increase of ionic contribution to the dielectric constant in different glass groups, e.g., the large g is predominantly responsible in ZNbKLSNd glasses and the large λ_0^2 is predominantly responsible in other silicate oxide glasses.

3.3. *Effects of compositional properties on the dielectric characteristics of silicate oxide glasses*

In this section we discuss how OFS glasses, particularly ZNbKLSNd glasses exhibit high THz refractive indices by comparing their THz properties with those of other silicate oxide glasses. We thus focus on the contribution of ionic vibration to the dielectric property of glasses. Dielectric characteristics revealed by the present THz analysis should be correlated with the physical property of specific glasses. According to the simple diatomic chain oscillator model as we used in the THz analysis, the resonant wavelength λ_0 of the oscillator is determined by the mass of atoms and the interatomic force within the groups of atoms comprising the glass network. The resonant wavelength is given by [43,44]:

$$\lambda_0 = 2\pi c\sqrt{\frac{\mu}{D}}, \tag{13}$$

where c is the speed of light, μ is the reduced mass, and D is the force constant of cation-anion pair. The resonant oscillator in a silicate oxide glass presumably results from a low-frequency vibrational mode of O-Si-O chains in the glass network, but the particular modifiers and intermediates introduced in the glass structure will perturb the O-Si-O vibration. Hence the resulting low-frequency vibrational mode will depend strongly on the structure and composition

Optical Materials EXPRESS

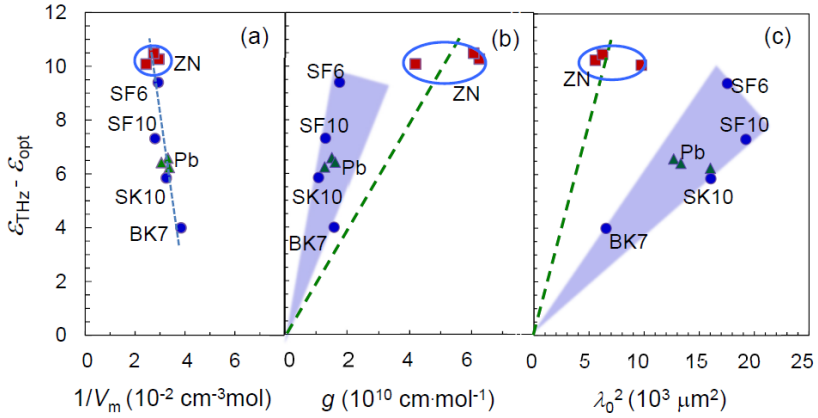

Fig. 8. The dielectric constant difference ε_{THz} - ε_{opt} as functions of $1/V_m$, g and λ_0^2 for silicate oxide glasses including PbNKLSNd (Pb) and ZNbKLSNd (ZN) glasses. A significant behavior difference is found between ZNbKLSNd glasses and other silicate oxide glasses.

of the glass. Thus, it can safely be assumed that the resonant wavelength λ_0 represents the dominant wavelength of all the low-frequency vibrational modes and that λ_0 can be used as a measure to know the variations in μ and/or D which are caused by the addition of modifiers and intermediates.

In silicate oxide glasses, as is shown in Fig. 8(c), λ_0 shows the largest value for SF series, the intermediate values for PbNKLSNd series and SK10 glass, and the smallest for ZNbKLSNd series and BK7 glass. We first discuss the effects of μ and D by comparing ZNbKLSNd glasses and SF glasses, both of which have similarly large dielectric constant differences up to 10. Here it can be noted that the THz refractive index has a one-to-one correspondence with the optical refractive index as shown in Fig. 4 and, in addition, that the optical refractive index, as well as the electronic polarizability as its cause, has an unambiguous, empirical relationships with the energy bandgap as have been reported for a variety of oxide glass materials [45–47]. Also, the energy bandgap of silicate oxide glasses is considered to be determined by the coupling strength of the dominant cation-anion pair. Taking into account that the optical bandgap energies of ZNbKLSNd glasses and SF glasses are not too much different (our visible region transmission experiment indicated the bandgap energy to be 3.18 eV for ZNbKLSNd05 glass, 3.15 eV for SF10 and 3.06 eV for SF6 glass), the cation-anion coupling strength and therefore the force constant D would not be significantly different for a first approximation. In consequence, the difference of λ_0 value between these two glass series is most likely resulted from the difference in the reduced mass μ. The SF series glasses involve large amount (molar fraction >50%) of modifier PbO and would contribute to effectively increase μ and eventually increase λ_0. On the other hand, ZNbKLSNd series glasses have considerable amount (molar fraction of 20%) of intermediate network former Nb_2O_5, and this would contribute to the effective decrease of the reduced mass due to the atomic number of Nb comparatively smaller than Pb, leading to a λ_0 value smaller than that for SF series. These tendencies are consistent with the observation in Fig. 8(c) as mentioned above. The inclusion of large amount of Nb_2O_5 is also considered to contribute to the increase of the refractive indices due to the high oxygen-to-cation ratio of Nb_2O_5 which can provide sufficient oxygen ions leading to the generation of non-bridging oxygens in the glass structure.

Optical Materials EXPRESS

When we turn to focus on a comparison between ZNbKLSNd glasses and BK7 glass both of which have similarly small λ_0 (Fig. 8(c)), BK7 glass has a much smaller g factor than ZNbKLSNd glasses (Fig. 8(b)). If we can assume that $g \propto 1/\mu$ (Eq. (10)) and $\lambda_0 \propto (\mu/D)^{1/2}$ Eq. (13) hold in these glasses (presuming no severe influence of other factors in Eq. (10)), the above feature (small g and small λ_0) is only possible when BK7 glass possesses a significantly large force constant D. Actually BK7 glass has small amount of additives and the bandgap energy estimated from the transmission data is as large as ~3.80 eV, indicating a stronger coupling and a larger D than in other oxide glasses. Consequently the small λ_0 in BK7 glass is attributable to a large force constant. This interpretation seems to provide qualitative agreement with the experimental results of dielectric properties in silicate oxide glasses.

Following the discussion based on Eqs. (10) and (13) as described above, a couple of comparatively distinctive features have been realized for certain groups of glasses: ZNbKLSNd glasses are characterized by small reduced mass primarily caused by the intermediates Nb_2O_5, SF series glasses have large reduced mass primarily due to modifiers PbO, and BK7 glass exhibits a large force constant due to strong cation-anion coupling. Other glasses (PbNKLSNd, SK10) likely locate in intermediate range in terms of the reduced mass and force constant.

The THz polarizability is linked with the optical polarizability through Eqs. (4) and (5) together with a parameter $a = P_i/P_e$ which seems to be characteristic to each group of glasses as is noticed in Table 1. The more ionic bonds are incorporated in the glass, the more ionic contribution would be expected to dominate the molar polalizability. Noticing that bonding of chalcogenide glasses is highly covalent and also silica has high covalency among silicate oxide glasses, it would be reasonable that these glasses have small a (0.37 for La:chalcogenide; 0.82 for silica, being smaller than for most of other silicate oxide glasses). The present hypothesis is likely supported by fairly high a values for BK7 (1.15) and SK10 (1.03) glasses in which alkaline cations such as Na^+, K^+, Ba^{2+} introduce ionic bondings. The a values found in FSO glasses (0.85-0.947 for ZNbKLSNd and 1.10-1.38 for PbNKLSNd series) are greater than that of silica. This seems to indicate the significance of ionic nature of the glass material, but further study is required for approaching to a precise mechanism of "a" parameter determination.

4. Conclusion

The THz dielectric properties of two (ZNbKLSNd and PbNKLSNd) series of OFS glasses have been characterized by THz-TDS and optical reflection measurements and discussed through a comparison with previously reported data on selected silicate oxide and chalcogenide glasses. The present OFS glasses, in particular, ZNbKLSNd glass has shown the highest THz (ν=0.5 THz) refractive index around 3.70. On the basis of Clausius-Mossotti relationship, THz and optical (λ=1.5 μm) dielectric constants have been correlated by a unified relationship using a parameter a which is defined by the ratio of the ionic polarizability to electronic polarizability for each glass series. This parameter a has been shown to be determined uniquely for each of the glass groups.

The dielectric constant difference estimated between the sub-THz and optical frequency ranges ($\varepsilon_{THz} - \varepsilon_{opt} = n_{THz}^2 - n_{opt}^2$), which correspond to the ionic contribution to the polarizability, has been analyzed in the sub-THz frequency region by using a simplified single oscillator model. The result has confirmed that the dielectric constant difference is well explained by the single oscillator model for all silicate oxide glasses examined, and the glass dependent factors such as the resonance wavelength λ_0 and amplitude factor g have been evaluated. Analysis has shown that the increase of the dielectric constant difference, which leads to high THz refractive index (e.g. SF series glasses), is supported by large λ_0 and small g in all silicate oxide glasses except ZNbKLSNd glasses. In contrast, ZNbKLSNd glasses have shown a distinctive feature with small λ_0 and large g.

Optical Materials EXPRESS

Effects of the glass composition have been discussed to understand the origin of large ionic polarizability in OFS glasses, particularly ZNbKLSNd glasses. The small λ_0 found in ZNbKLSNd glass has been attributed to the effects of large amount of intermediate network former Nb_2O_5 incorporated in the glass structure. Incorporation of Nb_2O_5, instead of heavy PbO in SF series glasses, effectively suppresses the reduced mass of cation-anion pair, leading to the small λ_0 as observed. It has also been suggested that the high oxygen-to-anion ratio of Nb_2O_5 helps introducing sufficient oxygen ions, which results in the enhancement of the total polarizability and THz refractive index.

In this study, THz dielectric properties of silicate oxide glasses, with a focus on OFS glasses, have been systematically interpreted in a unified approach. The high THz refractive index properties of OFS glasses, particularly ZNbKLSNd glasses, have been interpreted consistently with their physical properties.

Funding

Ministry of Science and Technology, Taiwan (# MOST 106-2112-M-007-022-MY2).

Acknowledgments

Dr. Doddoji Ramachari is thankful to Ministry of Science and Technology, Taiwan for the award of Postdoctoral Fellowship. The authors thank Chao-Kai Wang and Chun-Ling Yen for taking the THz-TDS data of the samples reported in this work.

Disclosures

The authors declare no conflicts of interest.

References

1. T. Nagatsuma, G. Ducournau, and C. C. Renaud, "Advances in terahertz communications accelerated by photonics," Nat. Photonics **10**(6), 371–379 (2016).
2. X.-C. Zhang and J.-Z. Xu, *Introduction to THz Wave Photonics* (Springer, 2010).
3. C. S. Yang, M. H. Lin, C. H. Chang, P. Yu, J. M. Shieh, C. H. Shen, O. Wada, and C. L. Pan, "Non-drude behavior in indium-tin-oxide nanowhiskers and thin films investigated by transmission and reflection THz time-domain spectroscopy," IEEE J. Quantum Electron. **49**(8), 677–690 (2013).
4. D. Saeedkia, Ed. *Handbook of Terahertz Technology for Imaging, Sensing and Communications* (Woodhead Publishing, 2013).
5. M. Tonouchi, "Cutting-edge terahertz technology," Nat. Photonics **1**(2), 97–105 (2007).
6. A. Quema, H. Takahashi, M. Sakai, M. Goto, S. Ono, N. Sarukura, R. Shioda, and N. Yamada, "Identification of potential estrogenic environmental pollutants by terahertz transmission spectroscopy," Jpn. J. Appl. Phys. **42**(Part 2, No. 8A), L932–L934 (2003).
7. G. C. Righini, I. Cacciari, A. Tajani, and M. Brenci, "Terahertz flexible waveguides: an overview," Proc. SPIE 7366, Photonic Materials, Devices, and Applications III **7366**, 73660Z (2009).
8. A. Zakery and S. R. Elliott, *Optical Nonlinearities in Chalcogenide Glasses and their Applications* (Springer, 2007).
9. R. C. Miller, "Optical Second Harmonic Generation in Piezoelectric Crystals," Appl. Phys. Lett. **5**(1), 17–19 (1964).
10. R. Li, F. Chen, X. Zhang, Y. Huang, B. Song, S. Dai, X. Zhang, and W. Ji, "Mid-infrared optical properties of chalcogenide glasses within tin-antimonyselenium ternary system," Opt. Express **25**(21), 25674–25688 (2017).
11. M. Zalkovskij, A. C. Strikwerda, K. Iwaszczuk, A. Popescu, D. Savastru, R. Malureanu, A. V. Lavrinenko, and P. U. Jepsen, "Terahertz-induced Kerr effect in amorphous chalcogenide glasses," Appl. Phys. Lett. **103**(22), 221102 (2013).
12. W. Shi, M. Leigh, J. Zong, and S. Jiang, "Single-frequency terahertz source pumped by Q-switched fiber lasers based on difference-frequency generation in GaSe crystal," Opt. Lett. **32**(8), 949–951 (2007).
13. Z. L. Sámson, S.-C. Yen, K. F. MacDonald, K. Knight, S. Li, D. W. Hewak, D.-P. Tsai, and N. I. Zheludev, "Chalcogenide glasses in active plasmonics," Phys. Status Solidi RRL **4**(10), 274–276 (2010).
14. J. E. Shelby, Introduction to Glass Science and Technology, 2nd edition (The Royal Society of Chemistry, 2005).
15. A. Jha, Inorganic Glasses for Photonics: Fundamentals, Engineering and Applications (John Wiley & Sons, 2016).
16. U. Strom, J. R. Hendrickson, R. I. Wagner, and P. C. Taylor, "Disorder-Induced Far Infrared Absorption in Amorphous Materials," Solid State Commun. **15**(11-12), 1871–1875 (1974).
17. U. Strom and P. C. Taylor, "Temperature and frefluency dependences of the far-infrared and microwave optical absorption in amorphous materials," Phys. Rev. B **16**(12), 5512–5522 (1977).

Optical Materials EXPRESS

18. T. J. Parker, J. E. Ford, and W. G. Chambers, "The Optical Constants of Pure Fused Quartz in the Far-Infrared," Infrared Phys. **18**(3), 215–219 (1978).
19. L. Ghivelder and W. A. Phillips, "Far Infrared Absorption in Disordered Solids," J. Non-Cryst. Solids **109**(2-3), 280–288 (1989).
20. S. Onari, K. Matsuishi, and T. Arai, "Far-Infrared Absorption Spectra and the Spatial Fluctuation of Charges on amorphous As-S and As-Se Systems," J. Non-Cryst. Solids **86**(1-2), 22–32 (1986).
21. D. Grischkowsky, S. Keiding, M. van Exter, and C. Fattinger, "Far-infrared time-domain spectroscopy with terahertz beams of dielectrics and semiconductors," J. Opt. Soc. Am. B **7**(10), 2006–2015 (1990).
22. M. C. Beard, G. M. Turner, and C. A. Schmuttenmaer, "Terahertz Spectroscopy," J. Phys. Chem. B **106**(29), 7146–7159 (2002).
23. M. Naftaly and R. E. Miles, "Terahertz Time-Domain Spectroscopy for Material Characterization," Proc. IEEE **95**(8), 1658–1665 (2007).
24. C.-K. Lee, C.-S. Yang, S.-H. Lin, S.-H. Huang, O. Wada, and C.-L. Pan, "Effects of two-photon absorption on terahertz radiation generated by femtosecond-laser excited photoconductive antennas," Opt. Express **19**(24), 23689–23697 (2011).
25. S. Kojima, H. Kitahara, S. Nishizawa, Y. S. Yang, and M. Wada Takeda, "Terahertz time-domain spectroscopy of low-energy excitations in glasses," J. Mol. Struct. **744-747**, 243–246 (2005).
26. E. P. J. Parrott, J. A. Zeitler, G. Simon, B. Hehlen, L. F. Gladden, S. N. Taraskin, and S. R. Elliott, "Atomic charge distribution in sodosilicate glasses from terahertz time-domain spectroscopy," Phys. Rev. B **82**(14), 140203 (2010).
27. M. Naftaly and R. E. Miles, "Terahertz time-domain spectroscopy of silicate glasses and the relationship to material properties," J. Appl. Phys. **102**(4), 043517 (2007).
28. S. Tsuzuki, N. Kuzuu, H. Horikoshi, K. Saito, K. Yamamoto, and M. Tani, "Influence of OH-group concentration on optical properties of silica glass in terahertz frequency region," Appl. Phys. Express **8**(7), 072402 (2015).
29. A. Ravagli, M. Naftaly, C. Craig, E. Weatherby, and D. W. Hewak, "Dielectric and structural characterisation of chalcogenide glasses via terahertz time-domain spectroscopy," Opt. Mater. **69**, 339–343 (2017).
30. S. B. Kang, M. H. Kwak, B. J. Park, S. Kim, H.-C. Ryu, D. C. Chung, S. Y. Jeong, D. W. Kang, S. K. Choi, M. C. Paek, E.-J. Cha, and K. Y. Kang, "Optical and Dielectric Properties of Chalcogenide Glasses at Terahertz Frequencies," ETRI J **31**(6), 667–674 (2009).
31. M. Zalkovskij, C. Z. Bisgaard, A. Novitsky, R. Malureanu, and D. Savastru, "Ultrabroadband terahertz spectroscopy of chalcogenide glasses," Appl. Phys. Lett. **100**(3), 031901 (2012).
32. D. Ramachari, C.-S. Yang, O. Wada, T. Uchino, and C.-L. Pan, "High-refractive index, low-loss oxyfluorosilicate glasses for sub-THz and millimeter wave applications," J. Appl. Phys. **125**(15), 151609 (2019).
33. D. Ramachari, L. R. Moorthy, and C. K. Jayasankar, "Optical absorption and emission properties of Nd^{3+}-doped oxyfluorosilicate glasses for solid state lasers," Infrared Phys. Technol. **67**, 555–559 (2014).
34. P. Manasa, D. Ramachari, J. Kaewkhao, P. Meejitpaisan, E. Kaewnuam, A. S. Joshi, and C. K. Jayasankar, "Studies of radiative and mechanical properties of Nd^{3+}-doped lead fluorosilicate glasses for broadband amplification in a chirped pulse amplification based high power laser system "," J. Lumin. **188**, 558–566 (2017).
35. "Borosilicate glass" (Pulles & Hanique B.V.) http://www.pulleshanique.com/02_borosilicate-glass.htm (last accessed April 12, 2019)
36. T. S. Izumitani, Optical Glass, (American Institute of Physics, 1986)
37. N.P. Bansal and R.H. Doremus, Handbook of Glass Properties, (Academic Press Inc. Ltd., 1986)
38. R. Buczynski, J. Pniewski, D. Pyszi, R. Stepien, R. Kasztelanic, I. Kujiawa, A. Filipkowski, A. J. Waddie, and M. R. Taghizadeh, "Dispersion management in soft glass all-solid photonic crystal fibres," Opto−Electronics Review **20**(3), 207–215 (2012).
39. C. Kittel, *Introduction to Solid State Physics*, 5th ed. (John Wiley and Sons, 1977), Chap. 13.
40. Mark Fox, *Optical Properties of Solids*, (Oxford University Press, 2001)
41. J. M. Ziman, *Principles of the Theory of Solids*, (Cambridge University Press, 1964)
42. W. G. Spitzer, R. C. Miller, D. A. Kleinman, and L. E. Howarth, "Far Infrared Dielectric Dispersion in $BaTiO_3$, $SrTiO_3$, and TiO_2," Phys. Rev. **126**(5), 1710–1721 (1962).
43. G. M. Barrow, *Physical Chemistry*, 4th ed., (McGraw-Hill, 1979)
44. Y. B. Saddeek, E. R. Shaaban, E. S. Moustafa, and H. M. Moustafa, "Spectroscopic properties, electronic polarizability, and optical basicity of Bi_2O_3–Li_2O–B_2O_3 glasses," Phys. B **403**(13-16), 2399–2407 (2008).
45. J. A. Duffy, "Chemical Bonding in the Oxides of the Elements: A New Appraisal," J. Solid State Chem. **62**(2), 145–157 (1986).
46. V. Dimitrov and S. Sakka, "Electronic oxide polarizability and optical basicity of simple oxides, I," J. Appl. Phys. **79**(3), 1736–1740 (1996).
47. V. V. Dimitrov, S.N. Kim, T. Yoko, and S. Sakka, "Third harmonic generation in PbO-SiO_2 and PbO-B_2O_3 glasses," J. Ceram. Soc. Jpn. **101**(1169), 59–63 (1993).